Chloride Complexation by Uranyl in a Room Temperature Ionic Liquid. A Computational Study

Alain Chaumont and Georges Wipff*

Laboratoire MSM, UMR CNRS 7551, Institut de Chimie, 4 rue B. Pascal, 67 000 Strasbourg, France

Received: April 11, 2008; Revised Manuscript Received: June 20, 2008

The stepwise addition of 1 to 4 Cl^- anions to the uranyl cation has been studied via potential of mean force (PMF) calculations in the [BMI][Tf_2N] ionic liquid based on the 1-butyl-3-methylimidazolium cation (BMI^+) and the bis(trifluoromethylsulfonyl)imide anion (Tf_2N^-). According to these calculations, the four Cl^- complexation reactions are favored and $UO_2Cl_4^{2-}$ is the most stable chloride complex in [BMI][Tf_2N]. The solvation of the different chloro-complexes is found to evolve from purely anionic (ca. 5 Tf_2N^- ions around UO_2^{2+}) to purely cationic (ca. 8.5 BMI^+ cations around $UO_2Cl_4^{2-}$), with onion-type alternation of solvent shells. We next compare the solvation of the $UO_2Cl_4^{2-}$ complex to its reduced analogue $UO_2Cl_4^{3-}$ in the [BMI][Tf_2N] and [$MeBu_3N$][Tf_2N] liquids that possess the same anion, but differ by their cation (imidazolium BMI^+ versus ammonium $MeBu_3N^+$). The overall solvation structure of both complexes is found to be similar in both liquids with a first solvation shell formed exclusively of solvent cations (about 9 BMI^+ cations or 7 $MeBu_3N^+$ cations). However, a given complex is better solvated by the [BMI][Tf_2N] liquid, due to hydrogen bonding interactions between Cl^- ligands and imidazolium-ring C−H protons. According to free energy calculations, the gain in solvation energy upon reduction of $UO_2Cl_4^{2-}$ to $UO_2Cl_4^{3-}$ is found to be larger in [BMI][Tf_2N] than in [$MeBu_3N$][Tf_2N], which is fully consistent with recent experimental results (*Inorg. Chem.* 2006, *45*, 10419).

Introduction

There is growing interest in room temperature ionic liquids ("IL"s) as "environmentally safe" (chemical stability, wide liquid temperature range, inflammability, negligible volatility and tunable physical properties) solvents for metal ions and their complexes involved in the nuclear industry.[1,2] Ionic liquids being typically composed of large organic cations M^+ (e.g., imidazolium, ammonium, pyridinium derivatives) combined with inorganic anions A^- are by essence polar and represent interesting media into which metallic cations and their complexes can be dissolved and further processed.[3] While the first generation of ILs was based on chloroaluminate anions that are highly air- and water-sensitive,[4−6] more recent studies used fluorine-containing hydrophobic anions.[7−9] This paper deals with the complexation properties of the uranyl cation UO_2^{2+}, which is of utmost importance in the context of nuclear fuel (re)processing. As shown by a recent study, its coordination in a [M][A] solution results from the competition between the X^- anion of the dissolved UO_2X_2 salt, the A^- anion of the IL, of added salts and, to a lesser extent, on the nature of the IL cation M^+.[10] For instance, addition of chloride salts to solutions of uranyl triflate, nitrate or perchlorate salts in the [BMI][Tf_2N] IL, based on the BMI^+ and Tf_2N^- ions (see Figure 1) leads to the formation of uranyl chloro complexes.[10] Recently, Sornein et al. showed that the tetrachlorouranyl $UO_2Cl_4^{2-}$ complex forms in the [BMI][Tf_2N] and [$MeBu_3N$][Tf_2N] ILs after dissolution of the $UO_2(Tf_2N)_2$ salt and addition of BMI^+Cl^- and $MeBu_3N^+Cl^-$ salts, respectively.[11] While the $UO_2Cl_4^{2-}$ complex has been characterized by X-Ray diffraction in the solid state [6,12,13] and by spectroscopy (EXAFS, UV−vis) studies in IL solution,[10,14] the stability of the corresponding mono to trichloro complexes remains to be assessed. Furthermore, there are so far no microscopic insights into the ion complexation process in a ionic liquid.

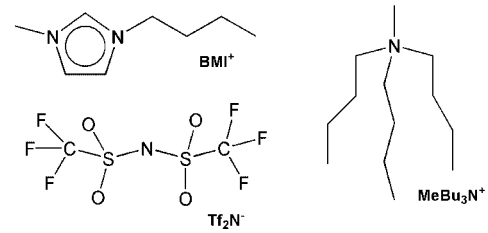

Figure 1. Ionic components of the simulated ILs.

Molecular dynamics simulations where all solute and solvent species are represented at the molecular level provide important insights into the structure and solvation properties of liquids.[15] Concerning ILs, most simulations concentrated so far on the neat liquids[16−21] or their mixtures with e.g. water, SC-CO_2, small organic molecules or organic liquids.[22−28] Our group initiated MD studies on the solvation of alkali and alkaline earth cations[29,30] and their complexes with macrocylic ligands,[31] and trivalent lanthanides, actinides,[10,30,32−36] focusing on the uranyl and uranium halo complexes. It was shown computationally that the "naked" UO_2^{2+} cation spontaneously captures Cl^- anions in a "basic" IL.[32] Also, comparing the UO_2^{2+}, 4 Cl^- complex with dissociated Cl^- anions to its $UO_2Cl_4^{2-}$ analogue with complexed anions in two ILs, we found that the former should be less stable, if one refers to the total internal energy U_{pot} of the solutions.[10] Similarly, the $EuCl_6^{3-}$ complex was predicted to be more stable than its dissociated analogue in IL solution.[37] These "predictions", although in agreement with experiment were qualitative, because of the high fluctuations in U_{pot}, and

* Corresponding author. E-mail: wipff@chimie.u-strasbg.fr.

10.1021/jp8031447 CCC: $40.75
Published on Web 08/28/2008

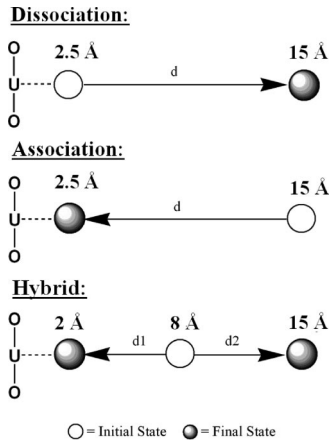

Figure 2. Schematic representation of the reaction coordinates used in the PMF calculations.

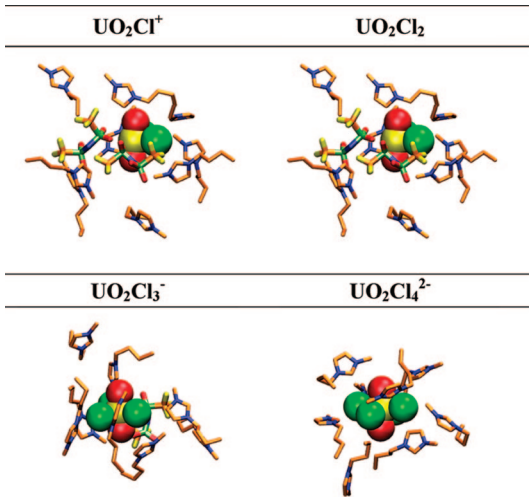

Figure 3. Snapshots of the first and second coordination shells of uranyl for the different $UO_2Cl_n^{2-n}$ complexes in [BMI][Tf_2N].

because U_{pot} is not a thermodynamic quantity. An alternative a priori more satisfactory computational approach is to calculate the free energy profile $\Delta G(d)$ for anion complexation in solution, as a function of a "reaction coordinate" d (potential of mean force "PMF" calculations).[15,38] Such simulations have been reported, e.g., for the complexation of cations[39−42] or anions[43] by macrocyclic ligands in aqueous and nonaqueous solvents, generally providing valuable insights into free energy changes while the reaction proceeds. Regarding the Cl^- complexation by uranyl, it is important to test whether the stepwise complexation of the anions is favored, i.e. ΔG_i is negative, and to investigate the height and nature of the corresponding barrier, if any. As the number of complexed Cl^- increases, uranyl formally evolves from cationic UO_2^{2+} and UO_2Cl^+ species to neutral UO_2Cl_2 and to $UO_2Cl_3^-$ anionic species, whose affinity for an additional Cl^- ligand is expected to gradually decrease, and it is thus important to gain insights into the corresponding free energy profiles. It should be recalled that the PMF calculations, based on the statistical perturbation theory require that the evolution from one state (uncomplexed ligand) to the other (complexed ligand) proceeds stepwise by small perturbations, and to collect a satisfactory statistics of the solvent configurations at all intermediate steps.[15,38,44] Ionic liquids are however quite viscous, and spectroscopic (e.g., time-resolved fluorescence spectra of polar molecular probes,[45−48] or pulse radiolysis experiments[49,50]), as well as simulation data (e.g., MD simulations of model or real probes)[28,51,52] indicate that the dynamics is characterized by a combination of very fast (subpicosend) and slow (multinanosecond) relaxation processes, the latter presumably involving the diffusion of IL ions. On the computational side, it is thus quite a challenge to test whether the PMF simulations correctly account for the stability of the tetrachloro $UO_2Cl_4^{2-}$ complex in the IL solution.

More specifically, we first report PMF calculations on the successive complexation of 4 Cl^- anions by UO_2^{2+} in the [BMI][Tf_2N] IL, with the main aim to describe the corresponding free energy changes and to characterize the structure and solvation of key intermediates or transition states. Next, inspired by the experimental investigations of Sornein et al.,[11] we want to gain insights into the effect of IL cation on the solvation of the uranyl complexes, and compare the solvation of the $UO_2Cl_4^{2-}$ complex and of its reduced $UO_2Cl_4^{3-}$ analogue in the [BMI][Tf_2N] versus [$MeBu_3N$][Tf_2N] IL.

Methods

Representation of the Potential Energy of the System. The systems were simulated by classical molecular dynamics (MD) using the modified AMBER 5.1 software[53] in which the potential energy U is described by a sum of bond, angle, and dihedral deformation energies and pairwise additive 1-6-12 (electrostatic + van der Waals) interactions between nonbonded atoms. Following most current studies on ILs, it is thus assumed that the ion···ion interactions are mainly electrostatic + steric in nature. See ref 54 for a review on the modeling of ionic liquids, and the Discussion section of this paper for the interactions with uranyl.

$$U = \sum_{bonds} k_b(b - b_0)^2 + \sum_{angles} k_\theta(\theta - \theta_0)^2 + \sum_{dihedrals}\sum_{n} V_n(1 + \cos(n\phi - \gamma)) + \sum_{i<j}\left[\frac{q_i q_j}{R_{ij}} - 2\varepsilon_{ij}\left(\frac{R^*_{ij}}{R_{ij}}\right)^6 + \varepsilon_{ij}\left(\frac{R^*_{ij}}{R_{ij}}\right)^{12}\right] \quad (1)$$

Cross terms in van der Waals interactions were constructed using the Lorentz−Berthelot rules. The BMI^+ cation parameters are taken from ref[18] while those of the Tf_2N^- anion stem from the work of Padua et al. and have been tested on the pure liquid properties.[20] The $MeBu_3N^+$ parameters[55] and UO_2^{2+} parameters[56] are taken from our previous work, while those of the Cl^- anions stem from the $AlCl_4^-$ anion.[18] The IL ions parameters and charges are given in Figure S1. The 1−4 van der Waals and the 1−4 Coulombic interactions were scaled down by a factor of 2.0. The solutions were simulated with 3D-periodic boundary conditions. Non-bonded interactions were calculated using a 15 Å atom based cutoff, with a reaction field "RF" correction to the Coulombic interactions. This correction assumes that the charge distribution within the sphere of cutoff radius interacts with the polarizable dielectric medium represented by a continuum and corrects for the discontinuities of the potential energy at the cutoff boundaries.[57]

Molecular Dynamics. The MD simulations started with random velocities and were performed, unless otherwise indicated, at 400 K to enhance the sampling. The temperature was monitored by coupling the system to a thermal bath using the Berendsen algorithm with a relaxation time of 0.2 ps. In

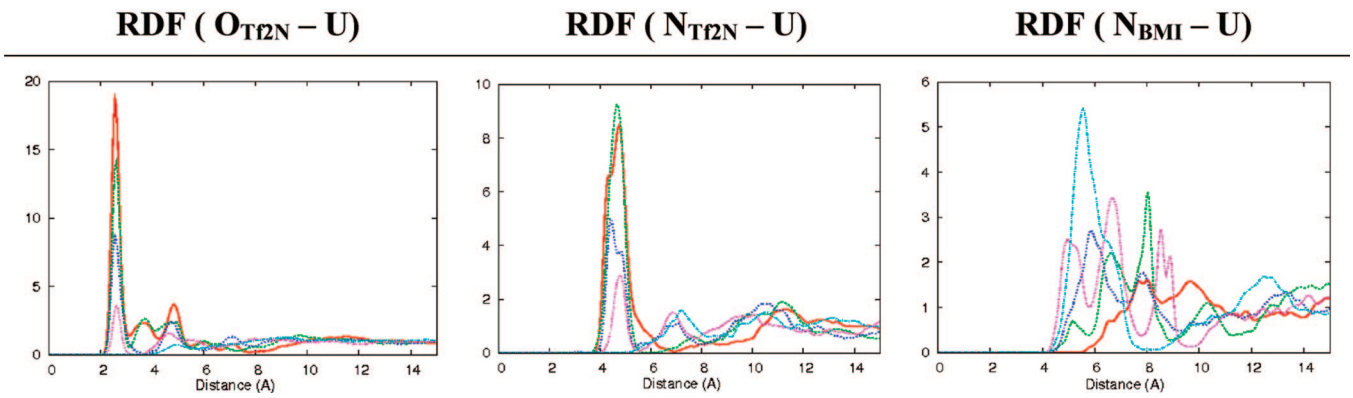

Figure 4. Solvent RDF's around the different $UO_2Cl_n^{2-n}$ complexes. (red, UO_2^{2+}; green, UO_2Cl^+; dark blue, UO_2Cl_2; pink, $UO_2Cl_3^-$, light blue, $UO_2Cl_4^{2-}$). A split representation is given in Figure S3.

TABLE 1: Characteristics of the [BMI][Tf_2N] Solvent RDF's around the $UO_2Cl_n^{2-n}$ Complexes: Coordination Number obtained by Integration of the First Peak of the RDF whose Maximum and Integration Distance (in Å) indicated in Parentheses

	U−O$_{Tf_2N}$	U−N$_{Tf_2N}$	U−N$_{BMI}$[a]
UO_2^{2+}	5.3 (2.55; 3.10)	4.8 (4.75; 5.90)	8.7
UO_2Cl^+	4.0 (2.60; 3.10)	4.1 (4.65; 6.90)	8.7
UO_2Cl_2	2.8 (2.55; 3.70)	2.1 (4.40; 5.35)	8.8
$UO_2Cl_3^-$	1.0 (2.60; 3.30)	1.0 (4.80; 5.50)	10.2
$UO_2Cl_4^{2-}$	*b*	*b*	8.5

[a] This first peak is ill-defined. [b] No Tf_2N- anion coordinates to the UO_2^{2+} cation.

the *NPT* simulations, the pressure was similarly coupled to a barostat with a relaxation time of 0.2 ps. All C−H bonds were constrained with SHAKE, using the Verlet leapfrog algorithm with a time step of 2 fs to integrate the equations of motion.

We first equilibrated "cubic" boxes of the pure ionic liquid, containing 200 BMI^+ cations and 200 Tf_2N^- anions, by repeated sequences of (i) heating the system at 500 K at constant volume for 0.5 ns, followed by (ii) 1 ns of dynamics at 300 K and a constant pressure of 1 atm and (iii) 1 ns of dynamics at 300 K and constant volume. The final box was simulated in the (*NVT*) ensemble for 2 ns at 300 K. The final density of the "dry" liquid was 1.49 kg/dm^3 in close agreement with the experimental value of 1.45 kg/dm^3.

For a given IL, all simulated systems contain the same number of particles, i.e. one UO_2^{2+} cation and four Cl^- anions as solute, removing two Tf_2N^- anions from the box to keep it neutral. The uncomplexed anions were initially placed at a U···Cl distance of 15 Å. Equilibration started with 1000 steps of steepest descend energy minimization, followed by 50 ps with fixed solutes ("BELLY" option in AMBER) at constant volume, and by 200 ps of constant volume without constraints, followed by 200 ps at a constant pressure of 1 atm coupling the system to a barostat with a relaxation time of 0.2 ps. Starting configurations for the PMF calculations were obtained after further 2 ns of MD in the *NVT* ensemble at a temperature of 400 K.

The MD trajectories were saved every 1 ps and analyzed with the MDS and DRAW software.[58] Typical snapshots were redrawn using the VMD software.[59] Insights into energy features were obtained by group component analysis, using a 15 Å cutoff distance and a reaction field correction for the electrostatics. The average structure of the solvent around the U atom was characterized by the radial distribution functions (RDFs) of the Tf_2N^- anions (N or O atoms) and BMI^+ or $MeBu_3N^+$ cations (N_{butyl} atoms) during the last 0.25 ns. The average coordination number (CN) of the solvent anion and cations and its standard deviation are calculated up to a cutoff distance of the first peak minimum of the RDF for the anions and up to 10 Å for the cations.

Free Energy Calculations. ***Potential of Mean Force "PMF" Calculations.*** We calculated the free energy profile for Cl^- anion complexation /dissociation as a function of the U···Cl distance *d*. Three different PMF's, starting from different configuration were considered (see Figure 2). (i) The dissociation PMF_{diss} where Cl^- is initially coordinated to the UO_2^{2+} cation, and *d* is linearly increased as a function of a λ parameter from 2.5 (λ = 1) to 15 Å (λ = 0). (ii) The association PMF_{ass} where Cl^- is initially dissociated from UO_2^{2+} (at 15 Å; λ = 1) and the distance d is linearly reduced as a function of λ to 2.5 Å (λ = 0). (iii) An hybrid PMF_{hyb} where the Cl^- ligand is initially at an intermediate position from the U atom (d = 8 Å) and from there two PMFs were calculated, one where the U−Cl distance is increased to 15 Å and a second where the U−Cl distance is decreased to 2 Å. In that hybrid PMF, there is less hysteresis between the end points of the PMFs than in the association or dissociation PMFs.

$$\Delta G = \Sigma \Delta G_\lambda = RT \log \langle \exp(U_\lambda - U_{\lambda+\Delta\lambda})/RT \rangle \qquad (2)$$

The change in free energy was calculated at each step using the free energy perturbation method (FEP) based on eq 2.[38] The transformation from the initial to the final state was achieved in 101 steps, i.e., with increments $\Delta\lambda$ of 0.01, corresponding to Δd = 0.125 Å. The changes of free energy ΔG were averaged from the forward ($\lambda + \Delta\lambda$) and backward ($\lambda - \Delta\lambda$) values. Different equilibration + data collection times at each step λ were tested. Exploratory tests used sampling times of 6 + 6 ps, 10 + 10 ps, 20 + 20 ps, and 30 + 30 ps, respectively at each window (see Figure S2). The final results reported in this paper were obtained using longer sampling, namely 150 + 150 ps at each window, thus requiring 30 ns for each type of PMF (association, dissociation, and hybrid). The corresponding free energy of complexation ΔG_c is calculated as the difference between ΔG (at d = 15 Å) and ΔG at the energy minimum (at $d \approx$ 2.5 Å).

Relative Free Energies of Solvation. The differences in free energies of solvation ΔG of $UO_2Cl_4^{2-}$ (complex-1) compared to its $UO_2Cl_4^{3-}$ reduced analogue (complex-2) were obtained

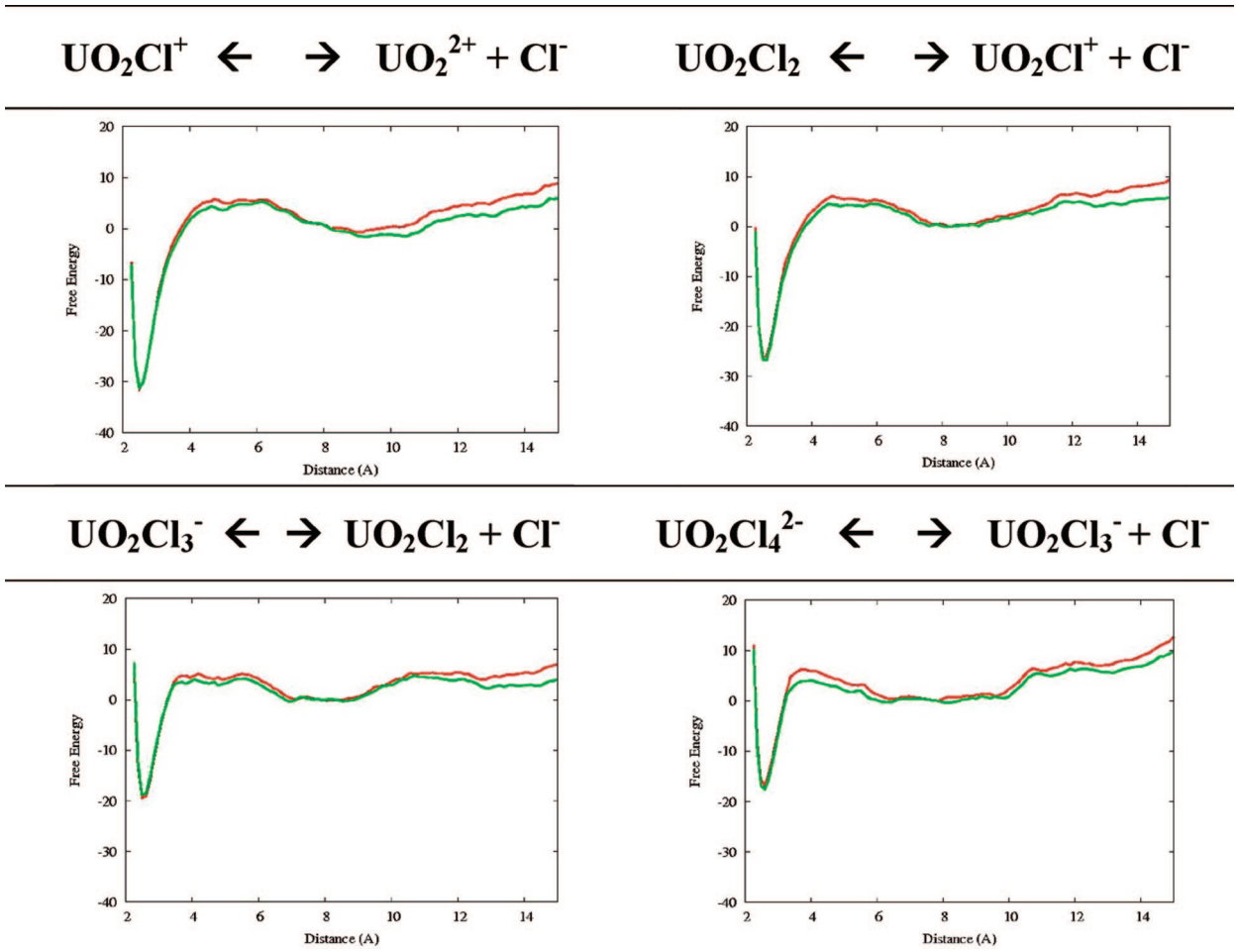

Figure 5. Free energy profiles upon the successive complexation of Cl^- anions to uranyl. Hybrid PMF calculations (Cl^- initially at 8 Å of the U atom, with 150 + 150 ps of sampling at each window), with forward (red) and backward (green) free energies. The corresponding full association PMF_{ass} and dissociation PMF_{diss} are given in Figures S4 and S5.

TABLE 2: Free Energies of Complexation (in kcal/mol) of One Cl^- Anion in [BMI][Tf_2N][a]

eq	reaction	ΔG_c
R1	$UO_2^{2+} + Cl^- \rightarrow UO_2Cl^+$	−38.7 (3.2)
R2	$UO_2Cl^+ + Cl^- \rightarrow UO_2Cl_2$	−33.9 (3.6)
R3	$UO_2Cl_2 + Cl^- \rightarrow UO_2Cl_3^-$	−24.7 (3.6)
R4	$UO_2Cl_3^- + Cl^- \rightarrow UO_2Cl_4^{2-}$	−28.4 (3.8)

[a] Averaged over the forward and backward calculations for the hybrid PMF_{hyb}. The hysteresis is given in parentheses. The corresponding values obtained from the association PMF_{ass} and dissociation PMF_{diss} are given in Tables S1 and S2.

by free energy perturbation calculations with the thermodynamic integration TI technique based on eq 3.[38]

$$\Delta G = \int \left\langle \frac{\partial U}{\partial \lambda} \right\rangle_\lambda d\lambda \qquad (3)$$

The transformation of one complex to the other was achieved via hybrid potential energy $U(\lambda)$ calculated using a linear combination of q charges of the initial complex ($\lambda = 1$) and the final one ($\lambda = 0$), i.e.

$$q_\lambda = \lambda q_1 + (1 - \lambda) q_2$$

Because all chloro ligands have been consistently modeled with −1 charges, the mutation involved the uranyl moiety, whose U charge was stepwise reduced from $q_U = 2.5$ e to $q_U = 1.5$ e, retaining the same q_O charges for simplicity. In principle, QM derived charges that take into account charge transfer from the anion to the metal are more satisfactory. However, recent calculations on UCl_6^{2-} complexes with the two types of charges have been shown to yield very similar results.[55]

The mutation of $UO_2Cl_4^{2-}$ to $UO_2Cl_4^{3-}$ was achieved in 21 steps, i.e. with increments $\Delta\lambda$ of 0.05. At each λ, we performed 20 ps of equilibration followed by 20 ps of data collection, and the changes of free energy ΔG were averaged from independent simulations from one complex to the other and vice versa. Concerning the treatment of electrostatics, unless otherwise indicated, all free energy calculations have been performed with the reaction field RF using a cutoff of 15 Å. In fact, the Ewald treatment of electrostatics requires the simulated system to be overall neutral, which is not the case here as the simulation involves a change of the total charge changes.

Results

In the first part we first briefly describe the structure and solvation of the different $UO_2Cl_n^{2-n}$ ($n = 0-4$) complexes in [BMI][Tf_2N]. This is followed by the free energy profiles for anion complexation and insights into their energy components. In the second part we compare the solvation of $UO_2Cl_4^{2-}$ and $UO_2Cl_4^{3-}$ complexes in two different ILs, namely [BMI][Tf_2N] and [$MeBu_3N$][Tf_2N].

I. Uranyl Complexes ($UO_2Cl_n^{2-n}$, $n = 0 - 4$) in [BMI][Tf_2N]. ***Solvation Structure around the Different $UO_2Cl_n^{2-n}$ Complexes.*** The solvation patterns around the various $UO_2Cl_n^{2-n}$ complexes display marked analogies to those previously ob-

TABLE 3: Energy Component Analysis (in kcal/mol) for the Initial State IS and Final State FS of Different PMF Calculations in [BMI][Tf_2N][a]

IS → FS		E_{Solute}	E_{Solv}	E_{IL}	U_{POT}
$UO_2^{2+} + Cl^- \rightarrow UO_2Cl+$	IS	−270 (−266)	−690 (−660)	5171 (5153)	4211 (4227)
	FS	−57 (−51)	−1022 (−991)	5313 (5303)	4234 (4261)
	Δ	−213	332	−142	−23
$UO_2Cl^+ + Cl^- \rightarrow UO_2Cl_2$	IS	−430 (−411)	−437 (−480)	5069 (5063)	4202 (4172)
	FS	−261 (−259)	−708 (−680)	5216 (5159)	4247 (4220)
	Δ	−169	271	−147	−45
$UO_2Cl_2 + Cl^- \rightarrow UO_2Cl_3^-$	IS	−520 (−522)	−330 (−337)	5037 (5061)	4187 (4202)
	FS	−425 (−433)	−451 (−433)	5093 (5119)	4217 (4253)
	Δ	−95	121	−56	−30
$UO_2Cl_3^- + Cl^- \rightarrow UO_2Cl_4^{2-}$	IS	−535 (−537)	−348 (−360)	5002 (5062)	4119 (4165)
	FS	−513 (−501)	−345 (−365)	5073 (4990)	4215 (4124)
	Δ	−22	−3	−71	−96

[a] Intrasolute energy ($E_{Solute,}$ involves the 4 Cl^- anions), solute-solvent interaction energy (E_{Solv}), intrasolvent energy (E_{IL}) and total potential energy U_{pot}. Averages taken over the last 150 ps of dynamics of the hybrid PMF_{hyb} run (starting from Cl^- at 8 Å, with 150 + 150 ps of sampling at each window). In brackets: energies calculated at the end points of the association PMF_{ass} for FS and of the dissociation PMF_{diss} for IS.

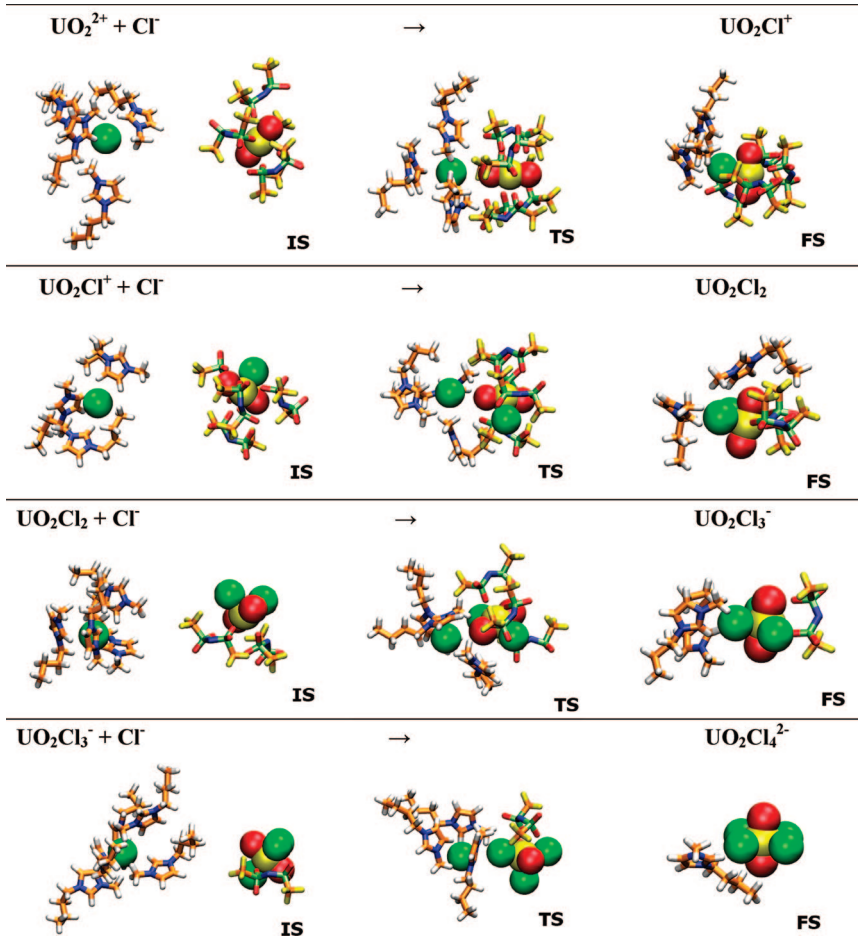

Figure 6. $UO_2Cl_n^{2-n} + Cl^- \rightarrow UO_2Cl_{n+1}^{1-n}$ reactions in [BMI][Tf_2N]: Snapshots along the reaction coordinate with selected solvent molecules. (IS = initial state; TS = transition state and FS = final state).

served in the [BMI][PF_6] ionic liquid,[33] as the first shell of the $UO_2Cl_n^{2-n}$ complexes with $n \leq 3$ is formed of solvent anions which directly coordinate to the U atom while the first solvation shell of the $UO_2Cl_4^{2-}$ complex is exclusively composed of solvent cations. See snapshots of the solvation around the different chloride complexes in Figure 3, solvent RDFs around the U atom in Figure 4, and the main characteristics of the RDFs in Table 1.

The number of (co)complexed Tf_2N^- anions decreases successively from 5 around UO_2^{2+}, to 4 around UO_2Cl^+, 2 around UO_2Cl_2, 1 around $UO_2Cl_3^-$, and 0 in the case of $UO_2Cl_4^{2-}$. Apart from the UO_2Cl_2 complex, where one Tf_2N^- anion is coordinated bidentate (with *cis*-chloro ligands), all other Tf_2N^- anions coordinate monodentate via one oxygen atom to the uranyl cation, at an average $U-O_{Tf_2N}$ distance of ca. 2.55 Å.

The various $UO_2Cl_n^{2-n}$ complexes are embedded in a "cage" formed by 9 to 10 BMI^+ cations forming a second shell around the complex. The solvent cation RDFs (Figure 3) show that this second cationic shell becomes tighter as the number of

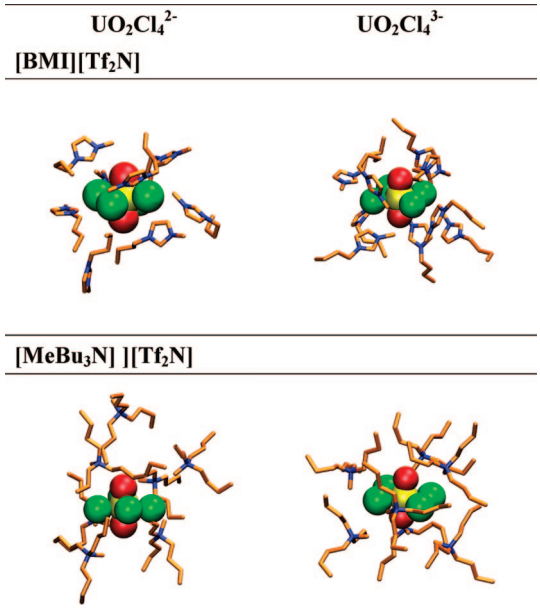

Figure 7. $UO_2Cl_4^{2-}$ and $UO_2Cl_4^{3-}$ in [BMI][Tf_2N] and [$MeBu_3N$][Tf_2N]: Typical snapshots of the first solvation shell around both complexes.

chloro-ligands increases, suggesting an improved solvation along the series. This results from the smaller size of the Cl^- anions compared to that of the Tf_2N^- anions and from the resulting stronger interactions of the BMI^+ cations with the Cl^-, compared to the Tf_2N^- ligands.

Free Energy Profiles for Chloride Complexation and Energy Component Analysis. We simulated the stepwise complexation of 4 Cl^- anions by the UO_2^{2+} cation according to reactions R1−R4:

$$UO_2^{2+} + Cl^- \rightarrow UO_2Cl^+ \quad \text{(R1)}$$

$$UO_2Cl^+ + Cl^- \rightarrow UO_2Cl_2 \quad \text{(R2)}$$

$$UO_2Cl_2 + Cl^- \rightarrow UO_2Cl_3^- \quad \text{(R3)}$$

$$UO_2Cl_3^- + Cl^- \rightarrow UO_2Cl_4^{2-} \quad \text{(R4)}$$

Such computations require that the reaction proceeds stepwise by small perturbations, and that the configurations of the different solvation states are sufficiently sampled at each intermediate step. According to the microreversibility principle, complexation and dissociation should occur via the same reaction pathways and display the same free energy profiles $\Delta G(d)$. Generally, the difference between backward and forward calculated free energies in a given run gives a rough idea of the quality of the sampling. In the case of ILs, such a criteria is however misleading, as can be seen from a comparison of different association PMF_{ass}'s obtained with 6 + 6 ps, 10 + 10 ps, 20 + 20 ps, and 30 + 30 ps of equilibration + averaging at each λ (Figure S2). For the latter PMFs, the difference between backward and forward calculated energies is low (a few kcal/mol), but the ΔG_{c1} free energy of complexation of the first Cl^- anion depends markedly on the sampling and evolves from a positive value with the 6 + 6 procedure, to nearly zero with the 10 + 10 and negative values for the 20 + 20 and 30 + 30 procedures, which indicates a lack of convergence due to unsufficient sampling. As mentioned in the introduction, ILs are viscous and have long relaxation times, and have no time to relax at each step along these PMF calculations. We thus decided to improve the sampling to 150 + 150 ps at each window, and we believe that this is sufficient to obtain more reliable free energy profiles. This was assessed first by computing three independent PMFs (Figure 2), corresponding respectively to (i) the complexation of a remote Cl^- ion (PMF_{ass}), or (ii) the dissociation of a Cl^- ligand from the complex (PMF_{diss}), or (iii) to use an hybrid procedure, with Cl^- at an intermediate position (PMF_{hyb}). Each PMF was started after 2 ns of MD equilibration. The resulting free energy profiles (see Figures 5, S4, and S5) are in qualitative accord with each other, indicating that the four complexation steps are favored. Futhermore, in order to check that a given state is similarly well represented by the different procedures, we compared selected energy components: the intrasolute energy (E_{Solute}), the solvent−solute interaction energy (E_{Solv}) and the intrasolvent energy (E_{IL}) at the end points (initial state IS and final state FS) of the different PMFs. The values for the hybrid PMF_{hyb} (see Table 3) are within statistical fluctuations (ca. 50 kcal/mol) close to those obtained from the association and dissociation PMFs, indicating that the systems have been sufficiently sampled along the PMFs. Unless otherwise specified, the results discussed in the following are those obtained via the hybrid pathway PMF_{hyb} (see Figure 5 and Table 2) which is a priori the most accurate. The results obtained via the full complexation PMF_{assn} and dissociation PMF_{diss} pathways yield similar conclusions and are given in Supporting Information (Figures S4 and S5 and Tables S1 and S2).

Typical snapshots taken along the PMF_{hyb} calculation are given in Figure 6. They show that the Cl^- does not approach the uranyl cation in its equatorial plane, but from "above", in order to reduce the repulsions with the Tf_2N^- equatorial ligands, via a SN_2 exchange type mechanism. The snapshots also illustrate the evolution of the solvation shells around Cl^- and the $UO_2Cl_n^{2-n}$ complex as the d distance decreases. In the initial state "IS", the uncomplexed Cl^- anion is fully surrounded by a shell of BMI^+ cations while the unsaturated $UO_2Cl_n^{2-n}$ complexes ($n < 4$) coordinated exclusively to Tf_2N^- anions ($U-O_{Tf_2N}$ interactions). In the final state (FS) the Cl^- anion is complexed by uranyl and both have lost about half of their solvation shell to coordinate directly to each other. The desolvation process of both moieties mainly occurs in the transition state (TS) where both solvation shells mix, with an interplay of $Cl^-\cdots{}^-Tf_2N(UO_2)$ repulsions, $(Cl)BMI^+\cdots{}^-Tf_2N(UO_2)$ and $Cl^-\cdots UO_2^{2+}$ attractions.

Structural variations along the reaction coordinate are reflected in the free energy profiles, as the Cl^- has first to pass a small energy barrier (transition state TS) before complexing to the uranyl cation. The height of this barrier is about 5 kcal/mol for each of the four reactions. The complexation free energies ΔG_c ($\Delta G_c = G_{FS} - G_{IS}$) are all markedly negative (they range from −25 to −40 kcal, depending on the reaction, see Table 2), indicating that the stepwise addition of 4 Cl^- ligands to the UO_2^{2+} is a highly exergonic process, and hence, the $UO_2Cl_4^{2-}$ complex is the most stable complex in the [BMI][Tf_2N] IL.

It is further interesting to compare the average total potential energies U_{pot} of the reactants (initial state IS) to the products (final state FS) of reactions R1−R4. The results in Table 3 show that the difference ΔU_{pot} ($\Delta U_{pot} = U_{FS} - U_{IS}$) is negative for all four reactions, thus following the same trends as the free energies reported above. Notice that the fluctuations of U are quite high (ca. 60 kcal/mol), however, while those for ΔG are quite smaller (a few kcal/mol, if one compares the three simulated PMFs). Dissecting ΔU_{pot} into the contributions of the intrasolute (ΔE_{solute}), the intrasolvent (ΔE_{IL}) and the solute/IL interactions ("solvation energy" ΔE_{solv}) shows that the ΔE_{solute} energy is negative for all four studied reactions, but decreases

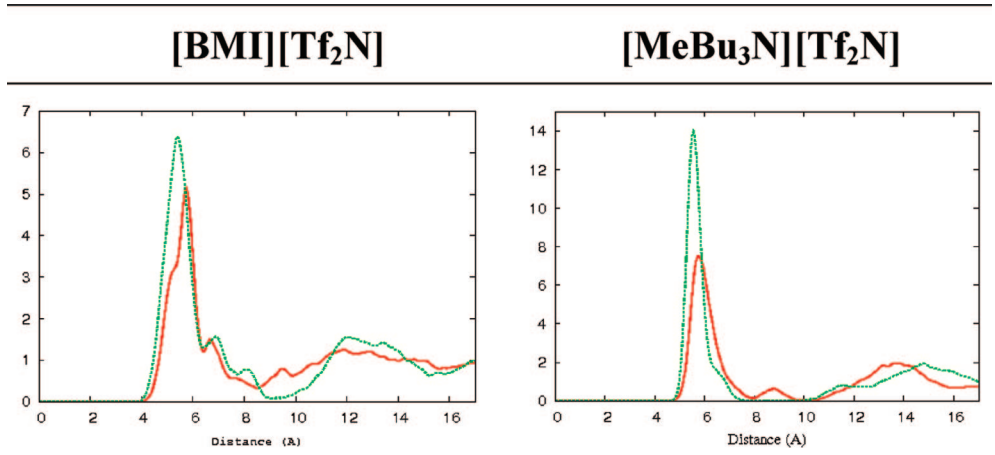

Figure 8. U...N(cation) RDF's around the $UO_2Cl_4^{2-}$ and $UO_2Cl_4^{3-}$ complexes.

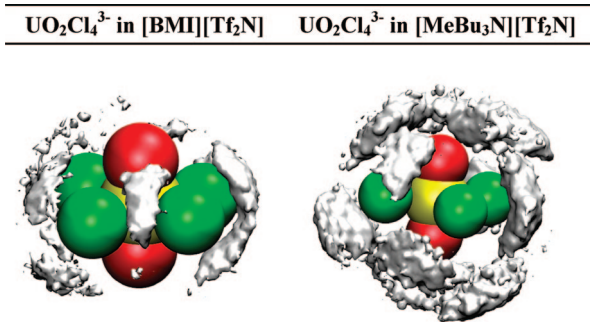

Figure 9. $UO_2Cl_4^{3-}$ in [BMI][Tf_2N] and [$MeBu_3N$][Tf_2N]: High proton density regions around the $UO_2Cl_4^{3-}$ complex in both solvents.

TABLE 4: $UO_2Cl_4^{2-}$ and $UO_2Cl_4^{3-}$ Complexes in [BMI][Tf_2N] and [$MeBu_3N$][Tf_2N] Solutions[a]

	E_{SOLV}	E_{COMP}	E_{IL}
	[BMI][Tf_2N] Solution		
$UO_2Cl_4^{2-}$	−271	−359	2773
$UO_2Cl_4^{3-}$	−383	−261	2789
	[$MeBu_3N$][Tf_2N] Solution		
$UO_2Cl_4^{2-}$	−239	−373	2806
$UO_2Cl_4^{3-}$	−302	−296	2811

[a] Solvation energy (ΔE_{SOLV}), intracomplex energy (ΔE_{COMP}), and intrasolvent energy (ΔE_{IL}) averaged over the last 500 ps of dynamics.

from reaction R1 to reaction R4, mainly due to increased repulsions between the equatorial Cl^- ligands. On the other hand, the ΔE_{solv} energy component is positive and decreases in magnitude from reaction R1 to R3, to become quasi-zero for reaction R4, in keeping with the enhanced second shell interactions described above. The desolvation of the Cl^- anion upon complexation makes ΔE_{solv} more positive, and this is more or less compensated by a better solvation of the uranyl complex when the number of its Cl^- ligands is increased. Usually, association of polar solutes is benefitial for the internal energy of the solvent itself (due to the release of first shell solvent molecules) and, accordingly, the ΔE_{IL} component also favors each of the four complexation reactions. There is however no regular trend of ΔE_{IL} along the series, due to the interplay of, among others, Tf_2N^-−Tf_2N^- repulsions (which increase when Tf_2N^- is displaced by Cl^- around the uranyl), BMI^+−BMI^+ repulsions (which increase when BMI^+ cations are released from the Cl^- solvation shell) and Tf_2N^-−BMI^+ attractions between IL ions released from the first shell of the solutes.

II. $UO_2Cl_4^{2-}$ and $UO_2Cl_4^{3-}$ in [BMI][Tf_2N] versus [$MeBu_3N$][Tf_2N] Liquids. In this section, we describe the solvation of the $UO_2Cl_4^{2-}$ and $UO_2Cl_4^{3-}$ complexes in two ionic liquids based on the same anion but on different cations, namely BMI^+ or $MeBu_3N^+$. Typical snapshots of the first solvation shell around both complexes are represented in Figure 7 and the corresponding radial distribution functions (RDF) around the U atom are given in Figure 8.

Similar solvation patterns are found around both complexes in the two different liquids, as their first solvation shell is composed exclusively of solvent cations. Integration of the first peak of the solvent RDFs up to their first minimum reveals that the first solvation shell of both complexes is composed of 9 BMI^+ cations in [BMI][Tf_2N] and of 7.0 $MeBu_3N^+$ cations in [$MeBu_3N$][Tf_2N]. If the number of solvent cations around both complexes is identical in a given liquid, the cations are however more attracted by the $UO_2Cl_4^{3-}$ than by $UO_2Cl_4^{2-}$ complex. As a result, the first solvation peak is shifted toward the U atom when the charge of the complex increases in magnitude. Marked differences are also seen in the solvation of the same complex in both liquids as BMI^+ cations can form hydrogen bonds with the chloride anions of the complexes while the ammonium cations cannot. This is illustrated by the region of highest proton density around the $UO_2Cl_4^{3-}$ complex (Figure 9). While the density of the imidazolium ring C−H protons mainly peaks in the equatorial plane of uranyl between two Cl^- ligands, the density of CH_3 protons of the various alkyl chains of the $MeBu_3N^+$ is delocalized around the whole $UO_2Cl_4^{3-}$ complex, indicating weaker and nonspecific interactions between $MeBu_3N^+$ and the complex.

These structural features are reflected in the solvent−solute attraction energies E_{solv} (see Table 4) that are more attractive for a given complex in [BMI][Tf_2N] than in [$MeBu_3N$][Tf_2N], in keeping with stronger hydrogen bonding interactions with imidazolium, compared to the ammonium cations. The ΔE_{solv} difference between the two liquids amounts to ca. 80 kcal/mol for $UO_2Cl_4^{3-}$ and 30 kcal/mol for $UO_2Cl_4^{2-}$, and is thus highest for the most charged complex. Comparing now one complex to the other in a given solvent, one sees that $UO_2Cl_4^{3-}$ is better solvated than $UO_2Cl_4^{2-}$ (ΔE_{solv} = −110 kcal/mol in [BMI][Tf_2N] and −60 kcal/mol in [$MeBu_3N$][Tf_2N]), mainly due to stronger Coulombic attractions with the former. Interestingly, the internal energy E_{Comp} of a given complex is not constant, but is lower in the ammonium than in the imidazolium based liquid (by at least 10 kcal/mol; see Table 4), indicating that the complex somewhat deforms to enhance its solvation, and this solvent-induced deformation is most pronounced, as

expected, for the most charged $UO_2Cl_4^{3-}$ complex in the [BMI][Tf_2N] liquid.

Further insights into the changes in solvation energy in a given liquid upon uranium reduction (from $UO_2Cl_4^{2-}$ to $UO_2Cl_4^{3-}$) can be obtained by the corresponding ΔG_{solv} changes in free energy of solvation. Indeed, the "alchemical transformation" of $UO_2Cl_4^{2-}$ to $UO_2Cl_4^{3-}$ gives negative ΔG_{solv} values, of −125 kcal/mol in [$MeBu_3N$][Tf_2N] and −158 kcal/mol in [BMI][Tf_2N], confirming that the most charged solute is best solvated in both liquids, as suggested by the simple Born equation model.[60] Furthermore, the ΔG_{solv} energy is higher in the [BMI][Tf_2N] than in the [$MeBu_3N$][Tf_2N] liquid, pointing to a marked solvent effect on the reduction potential of $UO_2Cl_4^{2-}$.

Discussion and Conclusion

We report in the first part of the paper the results of potential of mean force calculations on the stepwise complexation of Cl^- anions by uranyl in a ionic liquid, which is, to our knowledge, the first PMF study of ion complexation in an ionic liquid. We find that in that medium, the four reactions are favored, and that the $UO_2Cl_4^{2-}$ species should form preferentially. There are so far no thermodynamic complexation data on that system in an homogeneous IL phase, but the results are fully consistent with the experimental observation of the $UO_2Cl_4^{2-}$ complex when Cl^- anions (in the form of ammonium salts) are added to a solution of the $UO_2(Tf_2N)_2$ salt dissolved in the [BMI][Tf_2N] ionic liquid.[10,11] This contrasts with water solutions where uranyl has a very low affinity for chloride,[61,62] and that complex does not form at all. In fact, the $UO_2Cl_4^{2-}$ complex, well characterized in solid state structures [63−67] and in aprotic solvents like acetonitrile, acetone, tributylphosphate,[68,69] ionic liquids,[5,6,10,11,70,71] is intrinsically unstable. In the gas phase, according to quantum mechanical or force field calculations, it should lose one Cl^- ligand (see Figure S6), because the $UO_2Cl_3^-$ anion has no intrinsic affinity for another Cl^- anion. In the IL solution, however, this complexation is clearly favored. As discussed in ref 10, the "naked" uranyl cation is initially solvated by ca. 6 oxygen atoms from 5 Tf_2N^- anions in the IL solution, and the displacement of these anions by 4 Cl^- ligands is energetically favorable. An important stabilizing force comes from the solvation of the $UO_2Cl_4^{2-}$ complex, which is embedded inside a cage of BMI^+ cations, featuring an onion-type alternation of solvent shells, also observed by MD studies of ions in ionic liquids.[30,31,72,73] Such a solvation pattern is a specific feature of ILs, compared to traditional molecular solvents whose dipoles orient with respect to the ionic solute. We also note that the $UO_2Cl_4^{2-}$ complex, when observed in nonaqueous solutions, has often quaternary ammonium, imidazolium, or phosphonium counterions, which are potential components of ILs, and therefore stabilize the complex in these media.

The calculated free energies of complexation cannot pretend to be quantitative. In fact, following a procedure used so far to simulate most ionic liquids,[74] the PMF simulations are based on an empirical representation of the potential energy, assuming that the interactions between solvent ions, the uranyl cation and its Cl^- ligands are mainly steric and electrostatic in nature and described by pairwise additive 1−6−12 potentials. Improved treatments including polarization effects [75−77] and a fortiori quantum mechanical approaches like the Car−Parrinello method,[78−80] although a priori more accurate, are however presently precluded by the long relaxation times of the systems and related sampling issues. We note that electronic reorganization effects should be most pronounced for the complexes involving the "hard" uranyl cation, but the AMBER results compare well with QM (HF and DFT) results for the successive addition of 4 Cl^- to UO_2^{2+} in the gas phase (Figure S6). Similar agreements have already been reported on $EuCl_n^{3-n}$($n = 3-6$) and EuF_n^{3-n} ($n = 1-7$) complexes.[37] Other satisfactory AMBER versus QM comparisons involve the EuX_3 complexes with different X^- anions (triflate, Cl^-, F^-, and Tf_2N^-).[10] A recent study of the solvation of the UCl_6^{2-} complex in two ionic liquids, where the charges of the complex were either derived from QM calculations, or represented by integer numbers ($q_{Cl} = -1$ and $q_U = +4$) has shown that the solvation is quite the same with the two models. We thus feel that there is no major artifact with the force field representation of the uranyl complexes in solution.

Another important computational issue concerns the sampling of IL configurations around a given state of the solute, which is of particular concern with ILs, compared to traditional organic solvents or water. We tested different protocoles and sampling times, and concluded that running 150 + 150 ps of dynamics at each window at a temperature of 400 K samples sufficiently the solvent states. In fact, independent PMF simulations that started from different pre-equilibrated states converged to similar free energy profiles, and the main energy components (intracomplex, intrasolvent, and solute−solvent interaction energies) were within fluctuation errors similar for the end points of the different PMFs.

Another issue concerns the treatment of long-range electrostatics, and we feel that the RF method used for the PMF calculations is reasonable. As a test, we indeed recalculated the hybrid PMF_{hyb} of reaction R4, using the Ewald method, instead of the RF treatment of electrostatics. As mentioned above, this reaction is crucial because it concerns the formation of the $UO_2Cl_4^{2-}$ species that is intrinsically unstable. In fact, the result (Figure S7) is qualitatively the same as with the RF treatment, indicating that the process is exergonic (by ca. −25 kcal/mol). In that case, however, there is no clear barrier prior complexation.

The second part of the paper deals with the comparison of $UO_2Cl_4^{2-}$ and its redox states in two ILs based on a same anion, but with imidazolium versus quaternary ammonium cations. As found previously for the UCl_6^{2-} complex and its redox analogues,[81] the cationic component of the IL modulates the solvation and these tetrachloro uranyl anions: they are better solvated by imidazolium cations, in keeping with its H-bond donor properties, as observed in solid state structures.[81,82] The simulations also provide insights into energy features, confirming that a given anionic solute interacts more strongly with imidazolium than with ammonium based IL, and this effect is more pronouced for the $UO_2Cl_4^{3-}$ reduced species than for the oxidized $UO_2Cl_4^{2-}$ analogue, thus leading to solvent modulated redox potentials. These results are consistent with experimental observations.[11]

Taken together, the simulations contribute to our understanding of the effect of the environment on the coordination properties of an important cation (uranyl) and of the peculiar solvation properties of ionic liquids, compared to classical molecular polar solvents. We hope that they will stimulate experimental thermodynamic and kinetic studies.

Acknowledgment. The authors are grateful to IDRIS, CINES, Université Louis Pasteur, and GDR PARIS for computer resources, and to Etienne Engler for assistance. AC thanks the Alexander von Humboldt Foundation for a fellowship.

Supporting Information Available: Figure S1, AMBER types and atomic charges used for the simulation of the ILs, Figure S2, free energy profiles of the complexation of Cl^- by UO_2^{2+} cation in [BMI][Tf_2N], Figure S3, solvent RDF's around the different $UO_2Cl_n^{2-n}$ complexes, Figure S4, free energy profiles upon the successive addition of 4 Cl^- to UO_2^{2+}, Figure S5, free energy profiles upon the successive dissociation of 4 Cl^- from $UO_2Cl_4^{2-}$, Figure S6, $UO_2Cl_n^{2-n} + Cl^- \rightarrow UO_2Cl_{n+1}^{1-n}$ reactions in the gas phase, Figure S7, free energy profile for the complexation of Cl^- to $UO_2Cl_3^-$ in [BMI][Tf_2N], Table S1, free energies of complexation (in kcal/mol) of one Cl^- anion in [BMI][Tf_2N], and Table S2, free energies of complexation (in kcal/mol) of one Cl^- anion in [BMI][Tf_2N]. This material is available free of charge via the Internet at http://pubs.acs.org.

References and Notes

(1) Gutowski, K. E.; Bridges, N. J.; Cocalia, V. A.; Spear, S. K.; Visser, A. E.; Holbrey, J. D.; Davis, J. H.; Rogers, R. D. In *Ionic liquids IIIA: fundamentals, progress, challenges and opportunities. Properties and structure*; Rogers, R. D., Seddon, K. R., Eds.; American Chemical Society: Washington, DC, 2005; Vol. Chapter 3, p 33.

(2) Cocalia, V. A.; Gutowski, K. E.; Rogers, R. D. *Coord. Chem. Rev.* **2006**, *250*, 755–774.

(3) Welton, T. *Chem. Rev.* **1999**, *99*, 2071–2083.

(4) Deetlefs, M.; Seddon, K. R.; Shara, M. *Phys. Chem. Chem. Phys.* **2006**, *8*, 642–649.

(5) Dai, S.; Shin, Y. S.; Toth, L. M.; Barnes, C. E. *Inorg. Chem.* **1997**, *36*, 4900–4902.

(6) Hitchcock, P. B.; Mohammed, T. J.; Seddon, K. R.; Zora, J. A.; Hussey, C. L.; Ward, E. H. *Inorg. Chim. Acta* **1986**, *113*, L25−L26.

(7) Nikitenko, S. I.; Cannes, C.; Le Naour, C.; Moisy, P.; Trubert, D. *Inorg. Chem.* **2005**, *44*, 9497–9505.

(8) Bradley, A. E.; Hatter, J. E.; Nieuwenhuyzen, M.; Pitner, W. R.; Seddon, K. R.; Thied, R. C. *Inorg. Chem.* **2002**, *41*, 1692–1694.

(9) Visser, A. E.; Jensen, M. P.; Laszak, I.; Nash, K. L.; Choppin, G.; Rogers, R. D. *Inorg. Chem.* **2003**, *42*, 2197–2199.

(10) Gaillard, C.; Chaumont, A.; Billard, I.; Hennig, C.; Ouadi, A.; Wipff, G. *Inorg. Chem.* **2007**, 4815–4826.

(11) Sornein, M.-O.; Cannes, C.; Le Naour, C.; Lagarde, G.; Simoni, E.; Berthet, J.-C. *Inorg. Chem.* **2006**, *45*, 10419–10421.

(12) Perry, D.; Freyberg, D. P.; Zalkin, A. *J. Inorg. Nucl. Chem.* **1980**, *42*, 243–245.

(13) Zalkin, A.; Perry, D.; Tsao, L.; Zhang, D. *Acta Crystallogr.* **1983**, *C39*, 1186–1188.

(14) Binnemans, K. *Chem. Rev.* **2007**, *107*, 2592–2614.

(15) Allen, M. P.; Tildesley, D. J. *Computer Simulation of Liquids*; Clarendon Press: Oxford, U.K., 1987.

(16) Hanke, C. G.; Price, S. L.; Lynden-Bell, R. M. *Mol. Phys.* **2001**, *99*, 801–809.

(17) De Andrade, J.; Boes, E. S.; Stassen, H. In *Ionic liquids IIIA: fundamentals, progress, challenges and opportunities. Properties and structure*; Rogers, R. D., Seddon, K. R., Eds.; American Chemical Society: Washington DC, 2005; Vol. Chapter 9, pp 118−119.

(18) De Andrade, J.; Böes, E. S.; Stassen, H. *J. Phys. Chem. B* **2002**, *106*, 3546–3548.

(19) Canongia Lopes, J. N.; Deschamps, J.; Padua, A. A. H. In *Ionic liquids IIIA: fundamentals, progress, challenges and opportunities*; Rogers, R. D., Seddon, K. R., Eds.; American Chemical Society: Washington DC, 2005, Chapter 10, pp 134−135

(20) Canongia-Lopes, J. N.; Padua, A. A. H. *J. Phys. Chem. B* **2004**, *108*, 16893–16898.

(21) Liu, Z.; Wu, X.; Wang, W. *Phys. Chem. Chem. Phys.* **2006**, *8*, 1096–1104.

(22) Hanke, C. G.; Lynden-Bell, R. M. *J. Phys. Chem. B* **2003**, *107*, 10873–10878.

(23) Hanke, C. G.; Atamas, N. A.; Lynden-Bell, R. M. *Green Chem.* **2002**, *4*, 107–111.

(24) Hanke, C. G.; Johansson, A.; Harper, J. B.; Lynden-Bell, R. M. *Chem. Phys. Lett.* **2003**, *374*, 85–90.

(25) Lynden-Bell, R. M.; Kohanoff, J.; Popolo, M.; G, D. *Faraday Discuss* **2005**, *129/5*, 1–11.

(26) Shim, Y.; Duan, J.; Choi, M. Y.; Kim, H. J. *J. Chem. Phys.* **2003**, *119*, 6411–6414.

(27) Bursulaya, B. D.; Zichi, D. A.; Kim, H. J. *J. Phys. Chem.* **1996**, *100*, 1392–1405.

(28) Jeong, D.; Shim, Y.; Choi, M. Y.; Kim, H. J. *J. Phys. Chem. B* **2007**, *111*, 4920–4925.

(29) Vayssière, P.; Chaumont, A.; Wipff, G. *Phys. Chem. Chem. Phys.* **2004**, *7*, 124–135.

(30) Chaumont, A.; Engler, E.; Wipff, G. *Inorg. Chem.* **2003**, *42*, 5348–5356.

(31) Sieffert, N.; Wipff, G. *Phys. Chem. A* **2005**, *109*, 1106–1117.

(32) Chaumont, A.; Wipff, G. *Chem. Eur. J.* **2004**, *10*, 3919–3930.

(33) Chaumont, A.; Wipff, G. *Inorg. Chem.* **2004**, *43*, 5891–5901.

(34) Chaumont, A.; Wipff, G. *J. Phys. Chem B* **2004**, *108*, 3311–3319.

(35) Chaumont, A.; Wipff, G. *Phys. Chem. Chem. Phys.* **2005**, *7*, 1926–1932.

(36) Chaumont, A.; Wipff, G. *Phys. Chem. Chem. Phys.* **2006**, *8*, 494–502.

(37) Gaillard, C.; Billard, I.; Chaumont, A.; Mekki, S.; Ouadi, A.; Denecke, M.; Moutiers, G.; Wipff, G. *Inorg. Chem.* **2005**, *44*, 8355–8367.

(38) Kollman, P. *Chem. Rev.* **1993**, *93*, 2395–2417.

(39) Dang, L. X.; Kollman, P. A. *J. Am. Chem. Soc.* **1990**, *112*, 5716–5720.

(40) Marrone, T.; J, K. M.; Merz, J. *J. Am. Chem. Soc.* **1992**, *114*, 7542–7549.

(41) Marrone, T. J.; Merz, K. M. *J. Am. Chem. Soc.* **1995**, *117*, 779–791.

(42) van Eerden, J.; Briels, W. J.; Harkema, S.; Feil, D. *Chem. Phys. Lett.* **1989**, *164*, 370–376.

(43) Chaumont, A.; Engler, E.; Wipff, G. *Eur. J. Chem.* **2003**, *9*, 635–643.

(44) Zwanzig, R. *J. Chem. Phys.* **1954**, *22*, 1420.

(45) Aki, S. N. V. K.; Brennecke, J. F.; Samanta, A. *Chem. Comm.* **2001**, 413–414.

(46) Karmakar, R.; Samanta, A. *J. Phys. Chem. A* **2003**, *107*, 7340–7346.

(47) Ito, N.; Arzhantsev, S.; Heitz, M.; Maroncelli, M. *J. Phys. Chem. B* **2004**, *108*, 5771–5777.

(48) Ito, N.; Arzhantsev, S.; Maroncelli, M. *Chem. Phys. lett.* **2004**, *396*, 83–91.

(49) Funston, A. M.; Wishart, J. F. In *Ionic liquids IIIA; fundamentals, progress, challenges and opportunities. Properties and structure*; Rogers, R. D., Seddon, K. R., Eds.; American Chemical Society: Washington DC, 2005; Chapter 8, pp 102−103.

(50) Grodkowski, J.; Neta, P.; Wishart, J. F. *J. Phys. Chem. A* **2003**, *107*, 9794–9799.

(51) Znamenskiy, V.; Kobrak, M. N. *J. Phys. Chem. B* **2004**, *108*, 1072–1079.

(52) Kobrak, M. N.; Znamenskiy, V. *Chem. Phys. Lett.* **2004**, *395*, 127–132.

(53) Case, D. A.; Pearlman, D. A.; Caldwell, J. C.; Cheatham, T. E., III; Ross, W. S.; Simmerling, C. L.; Darden, T. A.; Merz, K. M.; Stanton, R. V.; Cheng, A. L.; Vincent, J. J.; Crowley, M.; Ferguson, D. M.; Radmer, R. J.; Seibel, G. L.; Singh, U. C.; Weiner, P. K.; Kollman, P. A. *AMBER5*; University of California: San Francisco, CA, 1997.

(54) Hunt, P. A.; Maginn, E. J.; Lynden-Bell, R. M.; Del Popolo, M. G. In *Ionic Liquids in Synthesis. Second, Completely Revised and enlarged Version*; Wasserscheid, P., Welton T., Ed.; Wiley-VCH: Weinheim, Germany, 2007; Vol. 1, pp 206−249.

(55) Schurhammer, R.; Wipff, G. *J. Phys. Chem. B* **2007**, *110*, 4659–4668.

(56) Guilbaud, P.; Wipff, G. *J. Mol. Struct. THEOCHEM* **1996**, *366*, 55–63.

(57) Tironi, I. G.; Sperb, R.; Smith, P. E.; van Gunsteren, W. F. *J. Chem. Phys.* **1995**, *102*, 5451–5459.

(58) Engler, E.; Wipff, G. In *Crystallography of Supramolecular Compounds*; Tsoucaris, G., Ed.; Kluwer: Dordrecht, The Netherlands, 1996; pp 471−476.

(59) Humphrey, W.; Dalke, A.; Schulten, K. *J. Mol. Graphics* **1996**, *14*, 33–38.

(60) Born, M. *Z. Phys.* **1920**, *1*, 45.

(61) Grenthe, I.; Fuger, J.; Konings, R. M.; Lemire, R. J.; Muller, A. B.; Nguyen-Trung Gregu, C.; Wanner, H. *Chemical Thermodynamics of Uranium*; North Holland: Amsterdam, 1992.

(62) Bühl, M.; Sieffert, N.; Golubnichiy, V.; Wipff, G. *J. Phys. Chem. B* **2008**, *112*, 2428–2436.

(63) Barker, T. J.; Denning, R. G.; Thorne, J. R. G. *Inorg. Chem.* **1987**, *26*, 1721–1732.

(64) Tanner, P. A. *J. Chem. Soc., Faraday Trans.* **1984**, *80*, 365.

(65) Flint, C. D.; Tanner, P. A. *Mol. Phys.* **1981**, *44*, 411.

(66) Görller-Walrand, C.; Vanquickenborne, L. G. *J. Chem. Phys.* **1972**, *57*, 1436.

(67) Danis, J. A.; Lin, M. R.; Scott, B. L.; Eichhorn, B. W.; Runde, W. *Inorg. Chem.* **2001**, *40*, 3389.

(68) Görller-Walrand, C.; De Houwer, S.; Fluyt, L.; Binnemans, K. *Phys. Chem. Chem. Phys.* **2004**, *6*, 3292–3298.

(69) Servaes, K.; Hennig, C.; van Deun, R.; Görller-Walrand, C. *Inorg. Chem.* **2005**, *44*, 7705–7707.

(70) Giridhar, P.; Venkatesan, K. A.; Srinivasan, T. G.; Rao, P. R. V. *Electron. Acta* **2007**, *52*, 3006–3012.

(71) Nockemann, P.; Servaes, K.; van Deun, R.; van Hecke, K.; Van Meervelt, L.; Binnemans, K.; Görller-Walrand, C. *Inorg. Chem.* **2007**, *46*, 11335–11344.

(72) Chaumont, A.; Wipff, G. *Phys. Chem. Chem. Phys.* **2003**, *5*, 3481–3488.

(73) Chaumont, A.; Wipff, G. *J. Mol. Liq.* **2006**, *131*−*132*, 36–47.

(74) Hunt, P. *Mol. Simul.* **2006**, *32*, 1−10and references cited therein.

(75) Yan, T.; Li, S.; Jiang, W.; Gao, X.; Xiang, B.; Voth, G. A. *J. Phys. Chem. B* **2006**, *110*, 1800–1806.

(76) Yan, T.; Burnham, C. J.; Popolo, M. G. D.; Voth, G. A. *J. Phys. Chem. B* **2004**, *108*, 11877–11881.

(77) Bagno, A.; Amico, F. D.; Saielli, G. *J. Mol. Liq.* **2007**, *131*, 17–23.

(78) DelPopolo, M. G.; Lyndel-Bell, R. M.; Kohanoff, J. *J. Phys. Chem. B* **2005**, *109*, 5895–5902.

(79) Kirchner, B.; Seitsonen, A. P.; Hutter, J. *J. Phys. Chem. B* **2006**, *110*, 11475–11480.

(80) Bühl, M.; Chaumont, A.; Schurhammer, R.; Wipff, G. *J. Phys. Chem. B* **2005**, *109*, 18591–18599.

(81) Nikitenko, S. I.; Hennig, C.; Grigoriev, M. S.; Le Naour, C.; Cannes, C.; Trubert, D.; Bossé, E.; Berthon, C.; Moisy, P. *Polyhedron* **2007**, *26*, 3136–3142.

(82) Deetlefs, M.; Hussey, C. L.; Mohammed, T. J.; Seddon, K. R.; van der Berg, J. A.; Zora, J. A. *Dalton Trans.* **2006**, 2334–2341.

JP8031447